Marquette University

e-Publications@Marquette

Physics Faculty Research and Publications

Physics, Department of

2-2010

The Metal Ion Requirements of *Arabidopsis thaliana* Glx2-2 for Catalytic Activity

Pattraranee Limphong
Miami University - Oxford

Ross M. McKinney
Miami University - Oxford

Nicole E. Adams
Miami University - Oxford

Christopher A. Makaroff
Miami University - Oxford

Brian Bennett
Marquette University, brian.bennett@marquette.edu

See next page for additional authors

Follow this and additional works at: https://epublications.marquette.edu/physics_fac

Part of the Physics Commons

Recommended Citation

Authors

Pattraranee Limphong, Ross M. McKinney, Nicole E. Adams, Christopher A. Makaroff, Brian Bennett, and Michael W. Crowder

The metal ion requirements of *Arabidopsis thaliana* Glx2-2 for catalytic activity

Pattraranee Limphong
Department of Chemistry and Biochemistry, Miami University, Oxford, OH

Ross M. McKinney
Department of Chemistry and Biochemistry, Miami University, Oxford, OH

Nicole E. Adams
Department of Chemistry and Biochemistry, Miami University, Oxford, OH

Christopher A. Makaroff
Department of Chemistry and Biochemistry, Miami University, Oxford, OH

Brian Bennett
Department of Biophysics, National Biomedical EPR Center, Medical College of Wisconsin, Milwaukee, WI

Michael W. Crowder
Department of Chemistry and Biochemistry, Miami University, Oxford, OH

Abstract

In an effort to better understand the structure, metal content, the nature of the metal centers, and enzyme activity of *Arabidopsis thaliana* Glx2-2, the enzyme was overexpressed, purified, and characterized using metal analyses, kinetics, and UV–vis, EPR, and ^{1}H NMR spectroscopies. Glx2-2-containing fractions that were purple, yellow, or colorless were separated during purification, and the differently colored fractions were found to contain different amounts of Fe and Zn(II). Spectroscopic analyses of the discrete fractions provided evidence for Fe(II), Fe(III), Fe(III)–Zn(II), and antiferromagnetically coupled Fe(II)–Fe(III) centers distributed among the discrete Glx2-2-containing fractions. The individual steady-state kinetic constants varied among the fractionated species, depending on the number and type of metal ion present. Intriguingly, however, the catalytic efficiency constant, k_{cat}/K_m, was invariant among the fractions. The value of k_{cat}/K_m governs the catalytic rate at low, physiological substrate concentrations. We suggest that the independence of k_{cat}/K_m on the precise makeup of the active-site metal center is evolutionarily related to the lack of selectivity for either Fe versus Zn(II) or Fe(II) versus Fe(III), in one or more metal binding sites.

Introduction

The glyoxalase system consists of two enzymes, lactoylglutathione lyase (Glx1) and hydroxyacylglutathione hydrolase (Glx2). In the presence of reduced glutathione, Glx1 forms *S*-(2-hydroxyacyl)glutathione (SLG) from 2-oxoaldehydes, and Glx2 then hydrolyzes these glutathione thioesters to form free hydroxyacids and glutathione [1]. This system apparently plays a critical role in cellular detoxification processes. It has received considerable attention as a possible antitumor and antimalarial target in animal systems [2–12]. Increased levels of Glx1 and Glx2 messenger RNA and protein have been detected in tumor cells, including breast carcinoma cells, and inhibitors of Glx1 and Glx2 have been shown to inhibit the growth of tumor cells in vitro [13, 14]. *Plasmodium falciparum* and the protozoan *Leishmania donovani* exhibit high rates of methylglyoxal formation and increased levels of Glx1 activity [15, 16]. Glx1 and Glx2 activity can inhibit the formation of hyperglycemia-induced advanced glycation end products, indicating that these enzymes may have a role in diabetes [17]. Finally, glyoxalase enzymes may also play a role in the pathogenesis of Alzheimer's disease [18, 19]. How the glyoxalase system can be linked with so many different disease states is not clear. However, Glx2 is thought to be the target of a prosurvival factor of the p53 family of transcription factors [20].

Glx2 exists as multiple isozymes. In humans, a single gene encodes both the mitochondrial and the cytoplasmic forms of Glx2 [21]. In *Arabidopsis thaliana*, five genes were identified and predicted to encode Glx2 isozymes (Glx2-1, Glx2-2, Glx2-3, Glx2-4, and Glx2-5) [22]. Glx2 enzymes have been purified and characterized from a number of sources, including humans and *Arabidopsis* [23, 24]. Glx2 belongs to the β-lactamase structural family of proteins [25] and has been shown to contain a dinuclear metal binding center [26–29]. Human Glx2 was reported to contain a dinuclear Zn(II) center (Fig. 1) [29]. *Arabidopsis* Glx2-5 appears to contain a dinuclear Fe(III)Zn(II) center, whereas Glx2-2 has been shown to bind Fe, Zn, and Mn [26–28]. The apparent flexibility of the Glx2-2 metal binding site has raised questions as to the nature of the native and/or active form of the enzyme and how changes in metal content affect the structure and activity of the enzyme. Previous studies on *A. thaliana* Glx2-2 have shown that the purified enzymes can bind widely varying amounts of metals despite use of the same growth media, purification column, and buffers [27, 28, 30]. In an effort to better understand why purified Glx2-2 samples contain different metal content and how changes in metal composition affect the structure and activity of the enzyme, recombinant *A. thaliana* Glx2-2 was overexpressed and purified in rich medium (Luria–Bertani). Each fast performance liquid chromatography (FPLC) column fraction containing Glx2-2 was analyzed for metal. Steady-state kinetic studies were conducted by measuring the hydrolysis rate of SLG to determine the relationship between metal content and catalytic activity. UV–vis, EPR, and ^{1}H NMR spectroscopic studies were used to characterize the structure of the metal centers in the column fractions containing Glx2-2.

Our data demonstrate that the different reported metal content of purified Glx2-2 samples can be explained by the choice of column fractions that were combined and concentrated. Furthermore, although the individual steady-state kinetic constants varied among the different species, the catalytic efficiency constant, k_{cat}/K_m, was relatively invariant. This result indicates that, at low substrate concentrations, the various forms of the enzyme are equally active in the elimination of SLG.

Fig. 1
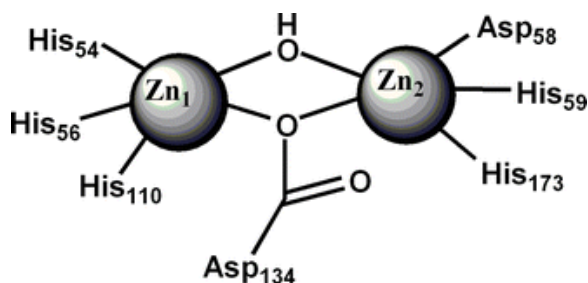
Active site of human hydroxyacylglutathione hydrolase (Glx2)

Materials and methods

Preparation of Glx2-2

The recombinant cytoplasmic Glx2 isozyme Glx2-2 from *A. thaliana* was prepared according to the procedure of Crowder et al. [24]. Cell cultures were grown at 310 K to an optical density at 600 nm of approximately 0.8–1.0 and were subsequently cooled to 288 K over 30 min. Protein production was then induced by the addition of 0.3 mM isopropyl-β-D-thiogalactopyranoside, and the cells were shaken at 288 K for 24 h. Glx2-2 concentrations were determined by measuring the absorbance at 280 nm and using a molar extinction coefficient of 34,180 $M^{-1} cm^{-1}$, as described previously [24].

Metal analyses

The metal content of Glx2-2 samples was determined using a Varian-Liberty 150 inductively coupled plasma spectrometer with atomic emission spectroscopy detection, as described previously [24].

Steady-state kinetics

Steady-state kinetic parameters (k_{cat}, K_m) were determined by measuring the hydrolysis rate of SLG in 10 mM 3-(*N*-morpholino)propanesulfonic acid (MOPS) buffer, pH 7.2, at 298 K with an Agilent 8453 diode-array UV–vis spectrophotometer, as previously described [24].

UV–vis spectroscopy

UV–vis spectra were recorded using an Agilent 8453 UV–vis spectrophotometer at 298 K. Glx2-2 concentrations were 300 µM, and the buffer was 10 mM MOPS, pH 7.2. Difference spectra (the spectrum of purple Glx2-2 minus the spectrum of yellow Glx2-2) were generated using Igor Pro version 4.0.5.1 (Wavemetrics).

EPR spectroscopy

The concentration of Glx2-2 in EPR samples was 0.7–1 mM, and the buffer was 10 mM MOPS, pH 7.2. Samples were pipetted into 4 mm outer diameter quartz EPR tubes and frozen by slow immersion of the EPR tubes into liquid nitrogen. EPR spectra were recorded with a Bruker EleXsys E600 spectrometer, equipped with an ER4116DM resonator operating at 9.63 GHz in the $B_0 \perp B_1$ mode, and an Oxford Instruments ESR-900 helium-flow cryostat. Spectra were collected with 1.8-G (0.18-mT) field resolution, at 2-mW microwave power, 10 K, and with 12-G (1.2-mT) field modulation amplitude at 100 kHz.

^{1}H NMR spectroscopy

^{1}H NMR spectra were collected with a Bruker Avance 500 spectrometer operating at 500.13 MHz, 298 K, a magnetic field of 11.7 T, a recycle delay (AQ) of 41 ms, and a sweep width of 400 ppm. Chemical shifts were referenced by assigning the H_2O signal the value of 4.70 ppm. A modified presaturation pulse sequence (zgpr) was used to suppress the proton signals originating from solvent. The concentration of protein was approximately 1 mM, and samples contained 10% D_2O or 90% D_2O for monitoring of solvent-exchangeable peaks.

Results

Overexpression and purification of *A. thaliana* Glx2-2

Glx2-2 was overexpressed in *Escherichia coli* cells grown in Luria–Bertani medium and purified at pH 7.2, as previously reported [24]. Cell extracts were applied to a 25-ml Q-Sepharose column and were eluted with a 0–500 mM NaCl gradient. Individual fractions of 8 ml were collected, and eight of these (fractions 18–26) (Fig. 2) were found to contain more than 95% pure Glx2-2. Fractions 18–19 were colorless, fractions 20–-23 were purple, and fractions 24–26 were yellowish-brown. One liter of culture yielded a total of 40–50 mg Glx2-2. Sodium dodecyl sulfate polyacrylamide gel electrophoresis showed that the protein product was more than 95% pure.

Fig. 2
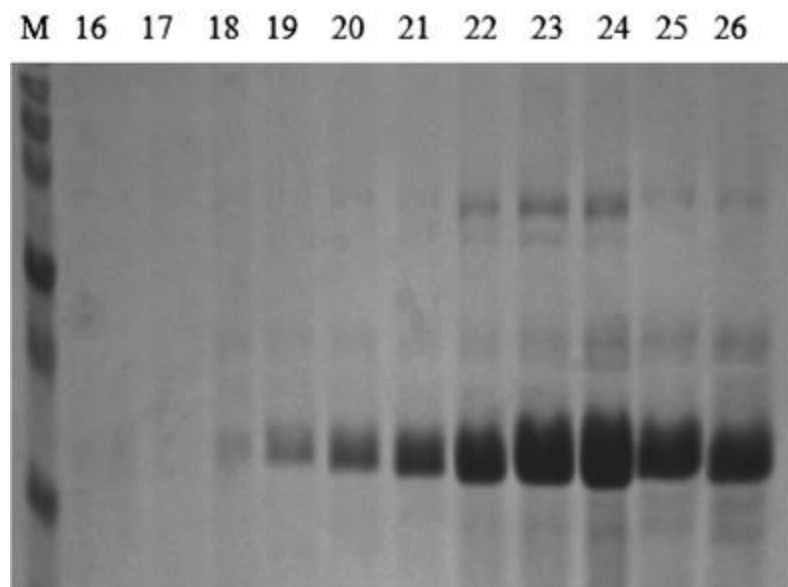
Sodium dodecyl sulfate polyacrylamide gel electrophoresis of column fractions containing Glx2-2. *Lane M* contains the molecular weight markers. Each column fraction was 8 ml

Metal content of FPLC fractions containing Glx2-2

The metal content of each FPLC fraction that contained Glx2-2 was measured using inductively coupled plasma atomic emission spectroscopy. The resulting enzyme from each fraction was shown to bind various amounts of Fe, Zn, and Mn; the metal analyses are shown pictorially in Fig. 3. It was found that the colorless fractions (18 and 19) and the purple fractions (20–23) contained Fe and Zn(II), with Fe-to-Zn ratios of about 1.5–2.1. The later, yellow fractions contained approximately equal amounts of Fe and Zn(II). None of the fractions contained significant amounts of Mn. The total metal content of the enzyme in the different fractions ranged from 0.26 equiv (fraction 18) to 1.94 equiv (fraction 22) (Table 1).

Fig. 3
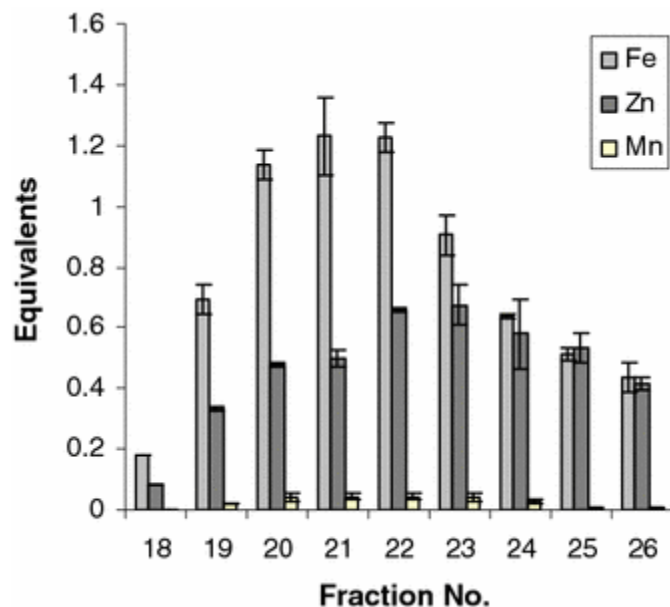
The metal content column fractions containing recombinant Glx2-2. *Error bars* represent the standard deviation of at least three replicates

Table 1 Metal content and steady-state kinetic constants for column fractions containing recombinant hydroxyacylglutathione hydrolase isozyme Glx2-2

Fraction	Fe (equiv)	Zn (equiv)	Mn (equiv)	Total (equiv)	k_{cat} (s^{-1})	K_m (µM)	k_{cat}/K_m (s^{-1} µM^{-1})
18	0.18 ± 0.01	0.08 ± 0.01	<0.01	0.26	65 ± 11	68 ± 21	0.96 ± 0.12
19	0.70 ± 0.05	0.34 ± 0.01	0.02 ± 0.01	1.06	210 ± 23	242 ± 37	0.87 ± 0.20
20	1.14 ± 0.05	0.48 ± 0.01	0.04 ± 0.01	1.66	447 ± 16	456 ± 25	0.98 ± 0.49
21	1.23 ± 0.13	0.50 ± 0.03	0.04 ± 0.01	1.77	406 ± 63	447 ± 208	0.91 ± 0.50
22	1.23 ± 0.05	0.66 ± 0.01	0.05 ± 0.01	1.94	526 ± 54	446 ± 81	1.2 ± 0.4
23	0.91 ± 0.06	0.68 ± 0.06	0.04 ± 0.01	1.63	558 ± 67	471 ± 106	1.2 ± 0.3
24	0.64 ± 0.01	0.58 ± 0.11	0.03 ± 0.01	1.25	543 ± 64	504 ± 118	1.1 ± 0.4
25	0.52 ± 0.02	0.54 ± 0.05	<0.01	1.07	564 ± 37	560 ± 143	1.0 ± 0.4
26	0.44 ± 0.05	0.42 ± 0.02	<0.01	0.87	426 ± 25	347 ± 113	1.2 ± 0.2

Steady-state kinetics

Previous studies have demonstrated that the preferred substrate for Glx2-2 is SLG [24].To evaluate how the kinetic constants of Glx2-2 are affected by the amount of Fe and Zn(II) present in the fractions, steady-state kinetic studies were conducted. The results are shown in Table 1. Figure 4 shows the dependence of k_{cat} and K_m on the metal content of Glx2-2 and the fraction number associated with the sample. The best correlation to Glx2-2 activity is with the Zn(II) content of the enzyme (Fig. 4a); the linear fit of k_{cat} against the number of equivalents of Zn(II) has a regression coefficient of 0.96. The kinetic behavior with Fe was more complex. The trend was that catalytic activity increased linearly with Fe until about 0.6 equiv Fe. Higher Fe content did not appear to further increase the activity and may even be inhibitory beyond 1 equiv Fe. One fraction, fraction 19, did not fit the trend; the reason for this is unknown, but the phenomenon was reproducible. Taken together, the activity data suggest that the optimum metal content for Glx2-2 activity is 1 equiv Zn and 1 equiv Fe (Fig. 4c). Given the very low levels of Mn, it is highly unlikely that Mn is associated with

catalytic activity. Another noteworthy correlation is that between k_{cat} and K_m (Fig. 4d). The value of k_{cat}/K_m sets a lower limit for the enzyme–substrate association rate [31]. The invariance of k_{cat}/K_m observed in Glx2-2 with different metal complements is striking and suggests an association-rate-limited catalytic reaction, which is consistent with results on rat erythrocyte Glx2 [32]. However, the value of k_{cat}/K_m, approximately 1×10^6 M^{-1} s^{-1}, is 10–100-fold lower than for classic diffusion-controlled enzyme catalysis, and k_{cat} and K_m are more generally seen to be statistically correlated [33]. Reaction velocities at low (much less than K_m) concentrations, as are more likely to be encountered in vivo, are dependent on k_{cat}/K_m rather than k_{cat} alone, and the evolutionary pressure therefore acts to optimize k_{cat}/K_m rather than k_{cat}; cf. [34, 35]. The kinetic data from Glx2-2 indicate that although metal ions promote activity, they interfere with substrate binding. Glx2-2 with a high metal content (two metal ions) is, therefore, an effective catalyst at high substrate concentrations, whereas at low substrate concentrations the catalytic efficacy is governed by k_{cat}/K_m, which is independent of bulk metal content over the range studied (0.26–1.94 equiv). A final observation is that although k_{cat}/K_m remains invariant over the wide range of metal bulk metal contents sampled, extrapolation of the fit to the k_{cat} data shown in Fig. 4 to zero metal content suggests that with zero metal content the activity of the enzyme is zero, or very close to it [34, 35].

Fig. 4
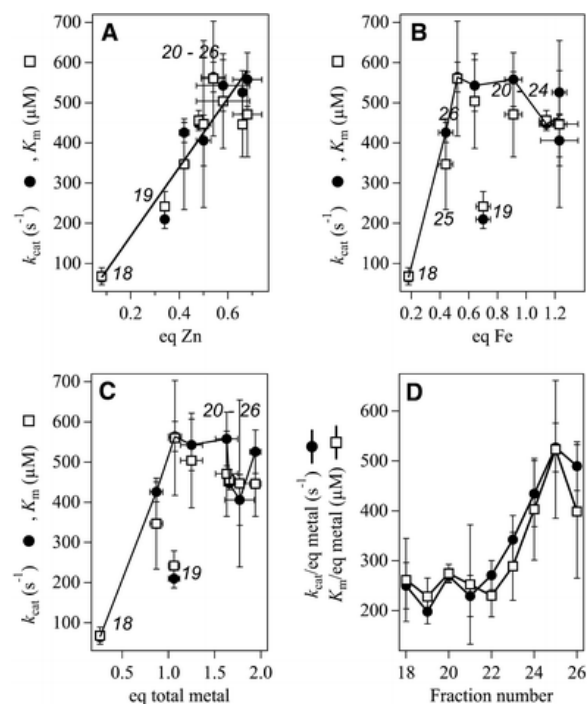
Kinetic parameters of Glx2-2 shown as a function of **a** Zn, **b** Fe, and **c** total metal content. **d** The kinetic parameters per equivalent metal ion for each fraction. *Labels* in **a**, **b**, and **c** indicate fraction numbers. *Circles* represent k_{cat} values, and *squares* represent K_m values

UV–vis spectroscopy

To obtain sufficient concentrations of enzyme for spectroscopic studies, several fractions, which contained similar complements of metal (Table 1), were pooled and concentrated. Specifically, fractions 20–23 were pooled, concentrated, and used in UV–vis studies. The UV–vis spectrum of the purple protein from fractions 20–23 showed a broad peak with maximal absorbance at 585 nm (Fig. 5, spectrum A). After 30 min, the purple protein turned yellow, and the UV–vis spectrum of this protein showed no discernable absorbance peak in the visible region (Fig. 5, spectrum B). The UV–vis difference spectrum of purple and yellow protein (the spectrum of

the purple protein sample minus the spectrum of the yellow protein sample) containing 1.20 equiv Fe and 0.55 equiv Zn(II) revealed the presence of a peak at 585 nm with an extinction coefficient of 310 $M^{-1}cm^{-1}$ (Fig. 5, spectrum C). The intensity of this peak suggests that it is due to a ligand field (d–d) transition of high-spin Fe(II), which should yield one ligand field transition. This assignment is consistent with the observed loss of color of the purple protein over time as Fe(II) is presumably oxidized to Fe(III). Given that the ligands of Fe(III) in Glx2-2 have moderate or weak field strengths and the fact that high-spin Fe(III) has a sextet ground electronic state [$^6A_{1g}$ if the Fe(III) has an octahedral geometry] [36], there are no spin-allowed transitions for Glx2-2 when it is bound to Fe(III). Nonetheless, we cannot completely rule out the peak at 585 nm being due to a ligand to metal charge transfer. The purple coloration of Glx2-2 is reminiscent of the purple acid phosphatases, which have a tyrosine that binds to an Fe(III), resulting in a tyrosinate to Fe(III) ligand to metal charge transfer band at approximately 550 nm (extinction coefficient of approximately 4,000 $M^{-1}cm^{-1}$) [37]. There are two tyrosines in the active site of human Glx2, which are conserved in Glx2-2, and one of the tyrosines (Tyr175) points directly towards the metal ion in the Zn_2 site [29]. However, both tyrosines are more than 5 Å away from the metal ions in the Zn_1 and Zn_2 sites [29]. Therefore, it is unlikely that the purple coloration of Glx2-2 is due to a tyrosinate to Fe(III) ligand to metal charge transfer band. There is also an intense shoulder at 310–350 nm (Fig. 5, spectra A, C) in the spectrum of the purple protein sample that has an extinction coefficient of more than 1,800 $M^{-1}cm^{-1}$. Given the intensity of this peak, we tentatively assign it to a histidine to Fe(III) ligand to metal charge transfer rather than to a higher-energy ligand field transition.

Fig. 5
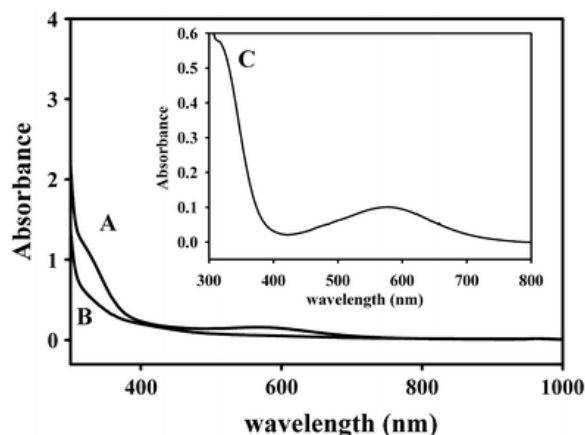
UV–vis spectra of Glx2-2 samples. *A* purple protein, fractions 20–23, *B* fractions 20–23 after 30 min, and *C* difference spectrum of spectrum *A* minus spectrum *B*. The enzyme concentration in the samples was 0.30 mM, and the buffer was 10 mM 3-(*N*-morpholino)propanesulfonic acid (MOPS), pH 7.2

EPR spectroscopy

EPR spectra of fractions of Glx2-2 were recorded, and illustrative spectra are presented in Fig. 6. The spectra were qualitatively similar in that four spectral features were observed to a lesser or greater extent in each of the fractions. At 3,600–4,500 G, signals characteristic of antiferromagnetically coupled Fe(II)–Fe(III) centers were observed. These signals from the colorless fractions (18 and 19; not shown) and the yellow fractions (24–26; Fig. 6, spectra E, F) were generally essentially single rhombic species with g_{eff} values of 1.93, 1.88, and 1.75. More complicated signals were observed in the purple fractions (20–23), containing an additional feature at g_{eff} = 1.95 that varied in intensity compared with that of the feature at g_{eff} = 1.92 (Fig. 6, spectra B, C). This more complex signal varied in form from fraction to fraction, and preparation to preparation, and also changed upon pooling and concentrating the purple fractions (Fig. 6, spectrum A). However, the same features were always present. The relative intensities of the g_{eff} = 1.75–1.95 signals also varied between individual fractions in

the same colorless, purple, or yellow group, and between preparations. The trend, however, was that the intensity (normalized for Fe content) of these signals was 2–5 times greater for the purple fractions than for the colorless or yellow fractions.

Fig. 6
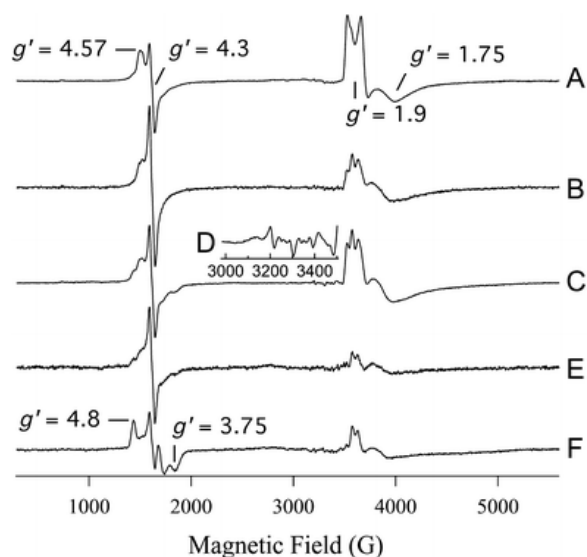
EPR spectra from Glx2-2. *A* pooled purple Glx2-2, *B* an early yellow fraction (fraction 24), *C* a late purple/early yellow fraction, *D* expanded region of *C* showing features due to Mn(II), *E* pooled yellow fractions (25 and 26), and *F* a late yellow fraction. Traces *A*, *B*, and *E* correspond to fractions from one chromatographic separation, and traces *C* (and *D*) and *F* correspond to another chromatographic separation. The spectral intensities for *A*–*C*, *E*, and *F* are shown normalized for spin concentration

Signals due to the trace Mn(II) content were small but observable, with characteristic 90-G hyperfine splitting. Figure 5, spectrum D shows an expanded view of the Mn(II) signal from a purple fraction of Glx2-2. The signals were unremarkable and not studied further.

The third type of signal that was observed was due to genuinely rhombic Fe(III). Two types of this signal were observed. The first type was characterized by a positive peak or shoulder at 1,505 G (g_{eff} = 4.57) and a negative peak or shoulder at 1,710 G (g_{eff} = 4.02), and is best resolved in the spectrum shown in Fig. 5, spectrum A. This signal was characteristic of the purple fractions and corresponds to an Fe(III) resonance in the M_s 3/2 Kramers doublet of S = 5/2, with E/D = 0.30. As well as being evident in the purple fractions, this signal was also present, but less well resolved and at lower intensity, in the colorless fractions. A second form of this type of signal exhibited features at 1,435 G (g_{eff} = 4.80), 1,735 G (g_{eff} = 3.97), and 1,835 G (g_{eff} = 3.75), and was observed in the yellow fractions and, in some preparations, in the later purple fractions along with the g_{eff} = 4.57–4.02 signal. This again corresponds to an Fe(III) resonance in the M_s 3/2 doublet of S = 5/2, but with E/D = 0.25. This signal was particularly well resolved in a fraction of yellow Glx2-2 from one particular preparation (Fig. 6, spectrum F), but was reproducibly observable along with other signals in other preparations (Fig. 6, spectra C, E). Upon exposure of the sample to air for 30 min, the E/D = 0.25 signal was extinguished and the E/D = 0.30 signal intensity diminished up to fivefold. Interestingly, no corresponding increase in the intensity of other signals was observed, suggesting that an antiferromagnetically coupled Fe(III)–Fe(III) center may result.

Finally, a signal at g_{eff} = 4.3 was always observed and is due to a subpopulation of highly *E*-strained Fe(III) that exhibits E/D = 1/3 [38]. This signal varied the most in intensity between fractions and preparations, and it is unclear whether it represents isolated Fe(III) in a mono Fe species of Glx2-2, or adventitiously bound Fe(III). The

assignment of this signal to a chemical species distinct from those responsible for the g_{eff} = 3.75–4.8 species arises from the fortuitous collection of a fraction in which the E/D = 0.25 signal was particularly well resolved (Fig. 6, spectrum F). Signals of the E/D = 0.25 type often include a component with g_{eff} = 4.3 because the strain-dependent envelope of E/D extends to E/D = 1/3, and the isotropic resonance for E/D = 1/3 appears with anomalously high intensity [38–40]. In the case of the spectrum shown in Fig. 5, spectrum F, though, the E/D = 0.25 signal is clearly very well resolved, and only a very small g_{eff} = 4.3 signal is present, indicating very little strain in E for this species. In addition, although the E/D = 0.30 signal was not seen without an accompanying g_{eff} = 4.3 signal, the relative intensities varied dramatically (compare spectrum A and spectrum B in Fig. 6). It is clear, then, that a separate Fe(III) component is responsible for the g_{eff} = 4.3 signal.

An attempt was made to quantify the spin content of the EPR signals, and the data from two preparations were pooled to estimate the paramagnetic contents. Although significant caution should be exercised in drawing conclusions from the apparent absolute number of spins [41], the overall EPR signal intensity tracked the Fe content reasonably well where the overall Fe content was high (Fig. 7). At lower total Fe, however, much of the Fe was EPR-silent, indicating either Fe(II) or a spin-coupled Fe(III)–Fe(III) center.

Fig. 7
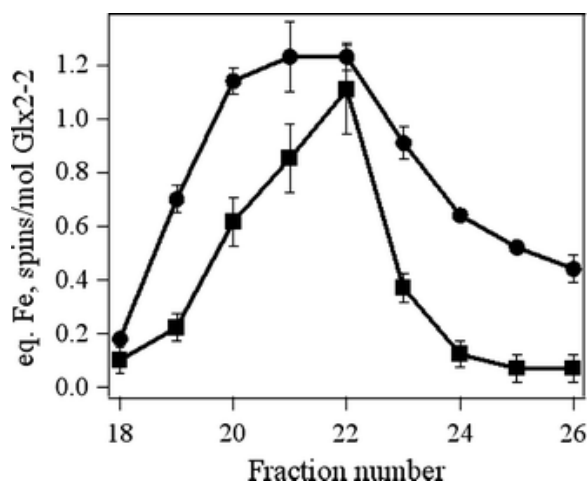
Fe and paramagnetic content of Glx2-2 fractions. *Circles* represent the number of equivalents of Fe and *squares* represent the number of spins per molecule of Glx2-2

^{1}H NMR spectroscopy

To probe further the metal binding sites of Glx2-2 in different column fractions, ^{1}H NMR spectra were obtained for (1) purple Glx2-2 (pooled/concentrated fractions 20–23), (2) oxidized, yellow Glx2-2 (pooled/concentrated fractions 20–23), and (3) pooled fractions 25–26 (Fig. 8). The ^{1}H NMR spectrum of purple Glx2-2 showed nine paramagnetically shifted resonances (peaks a–i) from 25 to 60 ppm (Fig. 8, spectrum A). It is very difficult to accurately integrate paramagnetically shifted peaks; however, we obtained the ^{1}H NMR spectrum of the same sample in 90% D_2O, and this spectrum offered insight into the number of protons associated with each peak. Peaks c and d completely disappeared in the 90% D_2O sample, suggesting that these peaks are due to one NH proton on a metal-bound histidine. Peaks b, f, h, and i, which did not change, are assigned to single non-solvent-exchangeable protons in the active site. Peak a decreased by 50% in the 90% D_2O sample, suggesting that this peak accounts for two protons, and one of these protons can be assigned to a third NH proton on a metal-bound histidine. In the 10% D_2O sample, peak e is most likely due to a single proton; however, peak e decreased by 50% in 90% D_2O, suggesting that it is due to a fourth NH proton on a metal-bound histidine. The fact that this peak did not disappear in the spectrum of the sample in 90% D_2O suggests that the solvent accessibility of this

histidine might be limited or that this peak is due to two protons—one that is solvent-exchangeable and one that is not. It is not clear how many protons make up peak g; however, this peak decreased by more than 50% in the spectrum of the Glx2-2 in 90% D_2O, suggesting the presence of a fifth NH proton on a metal-bound histidine. All of the peaks in this spectrum are relatively sharp, suggesting that the metal centers in this sample have short T_{1e} values. Given the fact five histidines are found in the Zn_1 and Zn_2 sites of Glx2-2, we can assign these shifted resonances to protons coupled to an antiferromagnetically coupled Fe(III)Fe(II) center, which is supported well by the EPR studies (Fig. 6, spectrum A) or to magnetically uncoupled Fe(II) centers.

Fig. 8
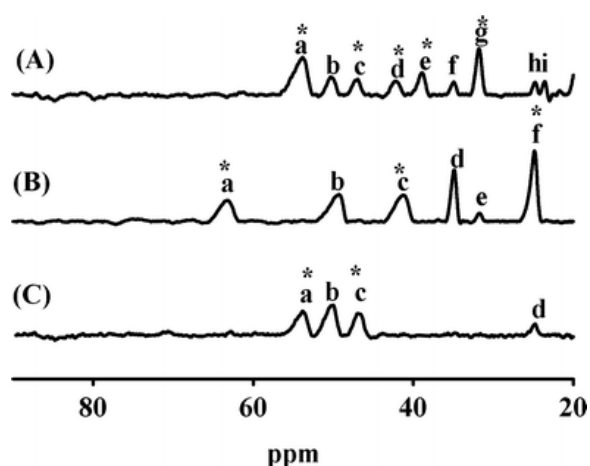
^{1}H NMR spectra of Glx2-2 samples. *A* purple protein, fractions 20–23, *B* fractions 20–23 after 30 min, and *C* fractions 25–26 of *Arabidopsis thaliana* Glx2-2 in 10 mM MOPS, pH 7.2, containing 10% D_2O. The enzyme concentrations in these samples were approximately 1 mM. *Asterisks* peaks that were solvent-exchangeable

The ^{1}H NMR spectrum of yellow, oxidized Glx2-2 (Fig. 8, spectrum B) showed six paramagnetically shifted peaks, and three of these peaks (a, c, and f) were solvent-exchangeable, again suggesting the presence of at least three or four NH protons on metal-bound histidines. The positions of these peaks were different from those observed in the ^{1}H NMR spectrum of pooled purple Glx2-2 (Fig. 8, spectrum A). Given that all of these samples contain mixtures of metal centers (see the EPR spectra in Fig. 6), it is not possible to make definitive assignments of protons coupled to specific metal centers; however, some general comments about the samples are possible. The relative broadness of peaks a, b, and c suggests that these protons are coupled to Fe(III) when they are part of an antiferromagnetically coupled Fe(III)Fe(II) center. The relatively sharper peaks d, e, and f can be assigned to protons coupled to a faster-relaxing metal ion, such as Fe(II). The ^{1}H NMR spectrum of fractions 25–26, which were yellow, showed only four paramagnetically shifted resonances (Fig. 8, spectrum C). The ^{1}H NMR spectrum of the same sample in 90% D_2O showed the complete loss of peak c and a 50% reduction of peak a, suggesting that peaks a, b, and c are due to two protons and that there are three histidines bound to Fe(II) in this sample. The mixture of metal centers in all of the Glx2-2 fractions prevents a more rigorous analysis of the ^{1}H NMR spectra, but these spectra are consistent with the Glx2-2 samples containing mixtures of metal centers and that the predominant, paramagnetic metal centers in each fraction are different.

Discussion

Glx2 has been structurally classified as a member of the Zn metallohydrolase family. This protein family includes other well known Zn metalloenzymes, such as the class B β-lactamases, sulfatases, transfer RNA maturase, rubredoxin oxidoreductase, and phosphotriesterase [42]. This superfamily of proteins, called the β-lactamase fold family, share a common tertiary fold (αββα) and a conserved metal binding motif (H–X–H–X–D). Previous

studies on several Glx2 enzymes from different sources have revealed a requirement of metal ions for catalysis. Human Glx2 and *E. coli* Glx2 were reported to contain a dinuclear Zn(II) center [29, 43]; however, plant mitochondrial Glx2 (Glx2-5) has been shown to contain an FeZn center [26], and plant cytoplasmic Glx2 (Glx2-2) can exist with a number of possible metal centers, including dinuclear Fe, FeZn, MnZn, and presumably dinuclear Zn(II) centers [27, 28]. Previous studies on Glx2-2 have also shown that Glx2-2 is isolated containing various amounts of metal ions despite the use of the same growth medium, purification columns, and buffers [27, 28]. In addition, the different preparations of Glx2-2 exhibited vastly differing steady-state kinetic constants [27, 28].

It was not clear from previous studies whether the catalytic activity of different Glx2-2 samples was due to a single species with a particular metal center or whether Glx2-2 enzymes containing different metal centers exhibit similar steady-state kinetic constants. The most obvious way to address these questions is to prepare metal-free Glx2-2 and stoichiometrically add metal ions back to generate analogs with specified metal centers. Unfortunately, Glx2-2 is not stable to the dialysis steps required to prepare metal-free enzyme when the most common direct addition method to prepare these samples is used [44]. In addition despite considerable efforts, we have not been able to prepare samples of Glx2-2 containing only one metal center using any of the known metal substitution/enrichment methods [27, 28, 45] (P. Limphong, C.A. Makaroff, and M.W. Crowder, unpublished results). We therefore analyzed individual column fractions to determine whether a Glx2-2 fraction containing a particular type of metal center and associated with catalytic activity could be isolated from forms containing other types of metal centers and lower, or zero, activity. The EPR studies conducted in this study demonstrated that Glx2-2 species containing different complements of metal centers could indeed be separated. Each of the column fractions containing Glx2-2 consisted of a mixture of metal centers. The NMR studies also showed that the different pooled/concentrated samples contained different NMR-active metal centers. For example, the predominant NMR-active center in fractions 20–23, which were purple, is an Fe(III)Fe(II) center that utilizes five histidines as metal binding ligands, whereas the predominant NMR-active center in fractions 25–26 probably contains an Fe(II) in the consensus Zn_2 site. This latter conclusion is consistent with the very low proportional content of Fe(III) in the yellow fractions, as indicated by EPR.

Three distinct Fe(III) species of Glx2-2 were detected by EPR. The $E/D = 0.30$ and $E/D = 0.25$ signals are from distinct species of Fe(III). Unlike the species responsible for the isotropic $g_{eff} = 4.3$ signal, the $E/D = 0.30$ and $E/D = 0.25$ species exhibit very low strains in the rhombic zero-field splitting and, hence, have very little geometrical heterogeneity. This indicates tight binding by rigid ligands in each case, as would be expected in the active site of an enzyme. The relative intensities of the $E/D = 0.30$ and $E/D = 0.25$ signals correlate well with Fe-to-Zn ratios of 2:1 and 1:1, respectively, and it is highly tempting to speculate that the $E/D = 0.3$ signal in the colorless and purple fractions is due to isolated Fe(III) in the active site, whereas the $E/D = 0.25$ signal is due to an Fe(III)–Zn(II) center. The apparently linear correlation of activity (k_{cat}) with Zn content and that with Fe content up to approximately 0.8 equiv but not beyond both suggest that the most catalytically active form of Glx2-2 at high substrate concentrations (i.e., $>K_m$) contains an Fe–Zn dinuclear center.

Taken together, the data in this study demonstrate:

1. Glx2-2 activity at high substrate concentration is associated with the presence of metal ions.
2. Glx2-2 species that contain different metal centers can coexist, including isolated Fe(II), isolated Fe(III), spin-coupled Fe(II)–Fe(III), and Fe(III)–Zn(II). Other possible, but unconfirmed, centers include EPR-silent Fe(II)–Fe(II), Fe(III)–Fe(III), Fe(II)–Zn(II), isolated Zn(II) and Zn(II)–Zn(II).
3. Discrete Glx2-2 metal-containing species are sufficiently kinetically stable that they can be separated and characterized.
4. k_{cat} measurements suggest that the most active form at high substrate concentration contains one Zn atom and one Fe atom.

5. k_{cat}/K_m, which determines the reaction rate at low substrate concentrations (much less than K_m), is *independent of metal ion content* in samples containing 0.26–2 equiv metal ions.

Finding 5 suggests some startling conclusions. Perhaps most startling is that if k_{cat}/K_m is assumed to be invariant down to zero metal content, then Glx2-2 would be expected to display activity as an apoenzyme. Extrapolation of the k_{cat} versus metal content data (Fig. 4), however, does not support the contention that the apoenzyme is active. Activity of the apoenzyme would require a different mechanism from the metal ion-catalyzed hydrolysis proposed for the metal-containing enzyme and related enzymes. No such alternative mechanism readily presents itself. Assuming, then, that the apoenzyme is *inactive*, the question then becomes one of how to explain the catalytic parameters at low metal ion content. The correlation between k_{cat} and metal ion content for 1 equiv Fe or less and/or 1 equiv Zn or less, and the invariance of k_{cat}/K_m, down to 0.26 equiv metal ion is intriguing. The kinetic data indicate that at low bulk metal content, Glx2-2 tightly binds substrate and, importantly, *that tightly bound substrate is ultimately hydrolyzed*, though more slowly than by Glx2-2 containing a higher bulk metal content. If Glx2-2 with the lowest metal content sampled, 0.26 equiv, is considered at the molecular level, then the obvious statement can be made that no individual molecule of Glx2-2 contains a quarter of a Zn or Fe ion. The population must consist of some apoenzyme, and some enzyme with either one or two metal ions bound. The kinetic data indicate that metal ions promote activity but interfere with substrate binding. In the mixed population, then, the metal-containing molecules are the catalytically active species, as indicated by the linear relationship between metal ion content and k_{cat}, whereas the apoenzyme has a higher affinity for the substrate, as indicated by K_m versus metal content. Substrate is efficiently bound by the inactive apoenzyme, therefore, but is only hydrolyzed by the metal-containing enzyme. However, for the binding of substrate by inactive apoenzyme to be reflected in the bulk kinetic constants, the substrate molecules that are bound by the inactive apoenzyme must ultimately be hydrolyzed. Further, the data indicate that they are hydrolyzed at a rate consistent with hydrolysis by the metal-ion-containing fraction of the population. Two mechanisms are consistent with this scenario. One is that substrate is exchanged between Glx2-2 molecules, with substrate ultimately being bound by a catalytically active metal-containing molecule of Glx2-2. Alternatively, metal ions are exchanged between Glx2-2 molecules, e.g., between naked metallated Glx2-2 and substrate-bound apo-Glx2-2. This latter scenario is reminiscent of a previous suggestion by Wommer et al. [46] that the binding of substrate increases the affinity of the some metallo-β-lactamases for metal. Further studies will be required to differentiate these candidate mechanisms.

From the conclusions derived, three important inferences can be made. The first is that Glx2-2 binds Fe and Zn(II) tightly and yet with very little preference between Fe(II), Fe(III), or Zn(II). This suggests an adaptability brought on by natural selection. Secondly, the enzyme's ability to catalyze the hydrolysis of substrate at high concentrations is correlated with the metal content and appears to be optimum with one Zn and one Fe atom. Thirdly, at very low substrate concentrations, the catalytic rate is *independent* of the number and type of metal ions, at least down to 0.26 equiv. An outstanding question is, then, why would an enzyme that is capable of a high level of catalytic activity when containing metal ions have evolved to tightly bind substrate in the apo form? An analysis of free-energy changes indicates that maximum catalytic rates at low enzyme concentration, the general situation in vivo, are achieved when K_m is within an order of magnitude of the substrate concentrations [47]. In the case of Glx2-2, the optimum species for catalysis are the metallated forms. However, K_m for these forms is high, rendering the metallated forms inefficient catalysts at low substrate concentration. It is possible, however, that when substrate is limited, a mixed population of apo-Glx2-2 and metallated Glx2-2 acts concertedly, with high-affinity apoenzyme binding substrate, which is then hydrolyzed either by substrate transfer to metallated Glx2-2 or by metal ion transfer from naked metallated Glx2-2 to substrate-bound apo-Glx2-2 [34, 35].

It is not clear if Glx2-2 is unique or if other Glx2's share this characteristic. Glx2-5, a putative mitochondrial Glx2 from *A. thaliana* [26], and Glx2-1, another β-lactamase fold protein that is not a Glx2 from *A. thaliana* [48], are eluted from chromatography columns in fractions that have different colors just like Glx2-2. On the other hand, column fractions of human Glx2 all contain the same metal content (P. Limphong, unpublished results). It is possible that human cells have evolved metal ion homeostatic mechanisms that more strictly control the concentration of metal ions in these cells as compared with plant cells. Future studies will address this hypothesis.

Abbreviations

FPLC: Fast performance liquid chromatography
Glx1: Lactoylglutathione lyase
Glx2: Hydroxyacylglutathione hydrolase
MOPS: 3-(*N*-Morpholino)propanesulfonic acid
SLG: *S*-(2-Hydroxyacyl)glutathione

References

1. Vander Jagt DL (1993) Biochem Soc Trans 21:522–527
2. Mannervik B (2008) Drug Metabol Drug Interact 23:13–27
3. Yang KW, Sobieski DN, Carenbauer AL, Crawford PA, Makaroff CA, Crowder MW (2003) Arch Biochem Biophys 414:271–278
4. Kalsi A, Kavarana MJ, Lu TF, Whalen DL, Hamilton DS, Creighton DJ (2000) J Med Chem 43:3981–3986
5. Tew KD (2000) Drug Resist Updates 3:263–264
6. Vince R, Brownwell J, Akella LB (1999) Bioorg Med Chem Lett 9:853–856
7. Kavarana MJ, Kovaleva EG, Creighton DJ, Wollman MB, Eiseman JL (1999) J Med Chem 42:221–228
8. Elia AC, Chyan MK, Principato GB, Giovannini E, Rosi G, Norton SJ (1995) Biochem Mol Biol Int 35:763–771
9. Thornalley PJ, Strath M, Wilson RJH (1994) Biochem Pharmacol 47:418–420
10. Chyan MK, Elia AC, Principato GB, Giovannini E, Rosi G, Norton SJ (1995) Enzyme Protein 48:164–173
11. Murthy NSRK, Bakeris T, Kavarana MJ, Hamilton DS, Lan Y, Creighton DJ (1994) J Med Chem 37:2161–2166
12. Norton SJ, Elia AC, Chyan MK, Gillis G, Frenzel C, Principato GB (1993) Biochem Soc Trans 21:545–548
13. Chyan MK, Elia AC, Principato GB, Giovannini E, Rosi G, Norton SJ (1994) Enzyme Protein 48:164–173
14. Rulli A, Carli L, Romani R, Baroni T, Giovannini E, Rosi G, Talesa V (2001) Breast Cancer Res Treat 66:67–72
15. Padmanabhan PK, Mukherjee A, Madhubala R (2006) Biochem J 393:227–234
16. Akoachere M, Iozef R, Rahlfs S, Deponte M, Mannervik B, Creighton DJ, Schirmer H, Becker K (2005) Biol Chem 386:41–52
17. Shinohara M, Thornalley PJ, Giardino I, Beisswenger P, Thorpe SR, Onorato J, Brownlee M (1998) J Clin Invest 101:1142–1147
18. Chen F, Wollmer MA, Hoerndli F, Munch G, Kuhla B, Rogaev EI, Tsolaki M, Papassotiropoulos A, Gotz J (2004) Proc Natl Acad Sci 101:7687–7692
19. Kuhla B, Boeck K, Schmidt A, Ogunlade V, Arendt T, Munch G, Luth HJ (2007) Neurobiol Aging 28:29–41
20. Xu Y, Chen X (2006) J Biol Chem 281:26702–26713
21. Cordell PA, Futers TS, Grant PJ, Pease RJ (2004) J Biol Chem 279:28653–28661
22. Maiti MK, Krishnasamy S, Owen HA, Makaroff CA (1997) Plant Mol Biol 35:471–481
23. Ridderstrom M, Saccucci F, Hellman U, Bergman T, Principato G, Mannervik B (1996) J Biol Chem 271:319–323
24. Crowder MW, Maiti MK, Banovic L, Makaroff CA (1997) FEBS Lett 418:351–354
25. Daiyasu H, Osaka K, Ishino Y, Toh H (2001) FEBS Lett 503:1–6
26. Marasinghe GPK, Sander IM, Bennett B, Periyannan G, Yang KW, Makaroff CA, Crowder MW (2005) J Biol Chem 280:40668–40675

27. Schilling O, Wenzel N, Naylor M, Vogel A, Crowder M, Makaroff C, Meyer-Klaucke W (2003) Biochemistry 42:11777–11786
28. Wenzel NF, Carenbauer AL, Pfiester MP, Schilling O, MeyerKlaucke W, Makaroff CA, Crowder MW (2004) J Biol Inorg Chem 9:429–438
29. Cameron AD, Ridderstrom M, Olin B, Mannervik B (1999) Structure 7:1067–1078
30. Zang TM, Hollman DA, Crawford PA, Crowder MW, Makaroff CA (2001) J Biol Chem 276:4788–4795
31. Place AR, Powers DA (1979) Proc Natl Acad Sci 76:2354–2358
32. Guha MK, Vander Jagt DL, Creighton DJ (1988) Biochemistry 27:8818–8822
33. Colquhoun D (1969) Appl Stat 18:130–140
34. Crowley PH (1975) J Theor Biol 50:461–475
35. Fersht AR (1974) Proc R Soc Lond B 187:397–496
36. Lippard SJ, Berg JM (1994) Principles of bioinorganic chemistry. University Science Books, Sausalito
37. Averill BA, Davis JC, Burman S, Zirino T, Sanders-Loehr J, Loehr TM, Sage JT, Debrunner PG (1987) J Am Chem Soc 109:3760–3767
38. Copik AJ, Waterson S, Swierczek SI, Bennett B, Holz RC (2005) Inorg Chem 44:1160–1162
39. Weisser JT, Nilges MJ, Sever MJ, Wilker JJ (2006) Inorg Chem 45:7736–7747
40. O'Toole MG, Bennett B, Mashuta MS, Grapperhaus CA (2009) Inorg Chem 48:7736–7747
41. Bou-Abdallah F, Chasteen ND (2008) J Biol Inorg Chem 13:15–24
42. Melino S, Capo C, Dragani B, Aceto A, Petruzzelli R (1998) Trends Biochem Sci 23:381-382
43. O'Young J, Sukdeo N, Honek JF (2007) Arch Biochem Biophys 459:20–26
44. Uotila L (1973) Biochemistry 12:3944–3951
45. Auld DS (1988) Methods for metal substitution, vol 158. Academic Press, New York, pp 71–79
46. Wommer S, Rival S, Heinz U, Galleni M, Frere JM, Franceschini N, Amicosante G, Rasmussen B, Bauer R, Adolph HW (2002) J Biol Chem 277:24142–24147
47. Cornish-Bowden A (1976) J Mol Biol 101:1–9
48. Limphong P, Crowder MW, Bennett B, Makaroff CA (2009) Biochem J 417:323–330